Turkish Journal of Engineering
https://dergipark.org.tr/en/pub/tuje
e-ISSN 2587-1366

Enhancing the seismic performance of high-rise buildings with lead rubber bearing isolators

Ahmet Hilmi Deringöl [*1], **Esra Mete Güneyisi**[1]

[1]*Gaziantep University, Department of Civil Engineering, Türkiye*

Keywords
Base isolation
High-rise building
Isolation period
Lead rubber bearing
Time-history analysis

Research Article
DOI: 10.31127/tuje.1026994

Received: 22.11.2021
Accepted: 10.04.2022
Published: 26.04.2022

Abstract

Recent earthquakes have enforced the engineering community to design seismically more efficient buildings through the energy dissipation systems. For this purpose, this paper investigates the seismic behavior of a high-rise building with a series of base isolation systems. Firstly, a 20-storey steel frame is selected as a fixed-base building, and then equipped with lead rubber bearings (LRBs). In the modelling of LRB, isolation period is alternatively varied as 4, 4.5, and 5 sec to evaluate the effectiveness of the isolator characteristic on the seismic performance of the high-rise base-isolated buildings. The seismic responses of the fixed-base and base-isolated buildings evaluated through a series of time-history analyses are performed using natural ground motion records. The analysis results are compared using engineering demand parameters such as storey displacement, isolator displacement, relative displacement, roof drift, interstorey drift ratio, absolute acceleration, base shear, base moment, input energy, and hysteretic curve. It is revealed that adjusting the isolation period in the design of LRB improved the seismic performance of the base-isolated high-rise steel buildings.

1. Introduction

The last devastating earthquakes in Turkey (e.g., Izmir 6.9 Mw, Malatya 5.7 Mw, Bingöl 5.9 Mw, Elazığ 6.8 Mw) reminded the expected major İstanbul earthquake that is to be 7+ Mw, resulted in the rupture of North Anatolian Fault, and caused thousands of fatalities and destructions [1]. Following the Marmara Earthquakes 7.4 Mw in 1999 that had struck off İstanbul, a series of legislative regulations/provisions on the seismic design codes were implemented through TEC (2007) [2] and TBEC (2018) [3]. The latter also includes the specifications for the base isolation systems (BIS). The increase of urbanization leads to the construction of high-rise buildings; however, they are much more susceptible to structural vibration under earthquakes and wind-induced seismic forces [4]. Likewise, the utilization of BIS for the retrofitting of existed buildings and designing of the newly structures significantly reduced the likelihood of casualties and structural damages during even major earthquakes and storms [5]. The idea behind the design of BIS is that decoupling the main structure from the foundation level and implementing a piece of flexible equipment made of either elastomeric or sliding bearings [6].

The BIS are generally categorized according to the energy dissipation mechanism namely rubber or friction-based bearings [7]. Among the former bearings, the lead rubber bearing (LRB) has favorable technique due to providing additional energy dissipation by lead core [8]. LRB is consisted of thin vulcanized steel plates, lead plug perpendicularly centered through the elastomeric rubber sheet as shown in Fig. 1 [9].

The isolator displacement demand of LRB depends on the shear modulus of the rubber material while the bearing capacity of the isolator is based on the vertical stiffness of the lead core consumed the external forces exerted by seismic actions [10]. The bilinear diagram represented in Fig. 2 can be constructed by two different models for rubber layer and lead plug of LRB. The former describes the linear viscoelastic behavior while the latter presents a linear elastic perfectly plastic model [11].

* **Corresponding Author**

*(aderingol@gmail.com) ORCID ID 0000-0002-2665-8674
(eguneyisi@gantep.edu.tr) ORCID ID 0000-0002-4598-5582

Cite this article

Deringöl, A. H., & Güneyisi, E. M. (2023). Enhancing the seismic performance of high-rise buildings with lead rubber bearing isolators. Turkish Journal of Engineering, 7(2), 99-107

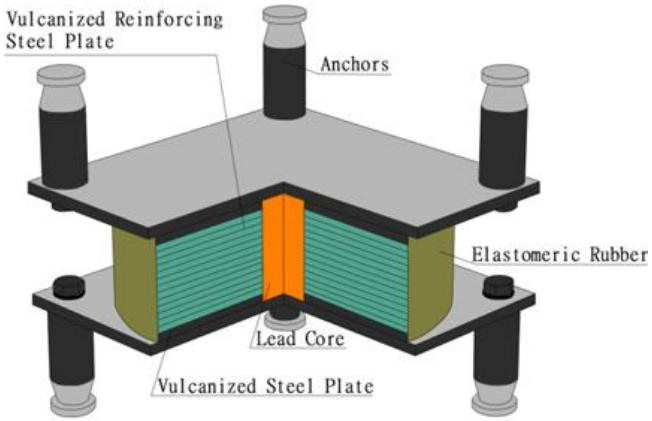

Figure 1. Typical configuration of LRB [9]

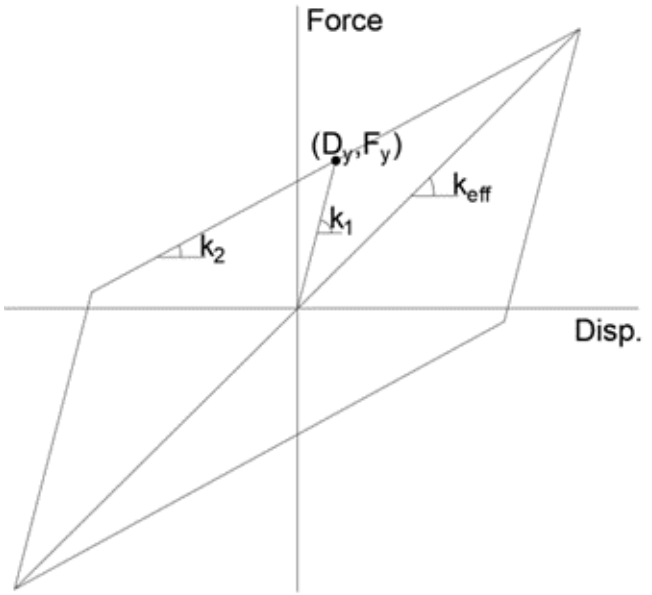

Figure 2. Hysteretic behavior of LRB isolator [11]

Many studies have been performed to the seismic performance of the base-isolated buildings with LRB. Kazeminezhad et al. [12], focused on the designing a new LRB model resisting all possible ground motions using performance point method in which a flowchart was presented to determine the isolation parameters by iterative procedure. The modified procedure decreased the base shear as 82 %. Deringöl and Güneyisi [13] evaluated the seismic performance of the regular and irregular frames with LRB considering such isolation parameters that effect the nonlinear response of the isolator. The use of proper LRB model significantly yielded the great interstorey drift reduction not only regular but also irregular frames. In the study of Shakouri et al. [14], the seismic performances of the base-isolated low and mid-rise buildings with LRB were evaluated trough time-history analyses considering the effect of ductility level and connection type. It was pointed out that both of them remarkably affected the maximum storey drift. But they recommended that the study should be extended for high-rise buildings. Ye et al. [15], proposed a design procedure based on the direct displacement method in order to satisfy the predefined displacement and drift values for the buildings with LRB. The flowchart was presented to simplify the application steps of the methods. The reliability of the design method was proved using nonlinear time-history analysis whether a series of benchmark buildings with LRB reaching the target values. Gupta et al. [16] investigated the effect of vertical force of the earthquakes on the base-isolated buildings with LRB. The drawbacks such as amplification on the isolator and residual displacements were overcome with additional shape memory alloy bearings. Habib et al. [17], studied on the irregularities (i.e., heavy and soft storey) of the low-rise base-isolated buildings with LRB considering various PGA/PGV ratios of near-fault earthquakes. The soft storey model with lower PGA/PGV ratios introduced the better nonlinear response of LRB. Altalabani et al. [18] proposed a new novel LRB model in which typical form of bearing (i.e., cylindrical) modified as rectangular and increased the number of lead core was evaluated by the seismic reliability analysis. The rectangular type LRB attenuated the first vibration mode and decreased occurrence of the structural damage. Zhang and Li [19] experimentally assessed the loading rate behavior of LRB by means of shear, compression, and relaxation mechanical tests. The stiffness of LRB increased when implemented the shear test with the higher loading rate. Deringöl and Güneyisi [20] evaluated the influence of the damping ratio on the seismic performance of the base-isolated steel frames with rubber bearing through the nonlinear analyses. It was shown that the increase in the effective damping ratio decreased the interstorey drifts.

It can be observed from the previous literature review that LRB is capable of improving the the seismic response of low and mid-rise buildings. On the other hand, there have been limited studies on the conformity of the high-rise buildings with base isolation systems examining the favorable isolation parameters which is still scarce subject especially for LRB. Therefore, this study focused on the effectiveness of LRB characterized with different isolation parameters to design seismically more effective base-isolated high-rise steel buildings. To this, 20-storey steel frame considered as a benchmark fixed-base building, and then upgraded with various LRB having a series of the isolation periods (e.g., T = 4, 4.5, and 5 sec) are produced to enhance the nonlinear response of the high-rise buildings. The seismic performance of the fixed-based and base-isolated buildings are evaluated through nonlinear analyses using a set of earthquakes to compare the seismic response of the high-rise buildings with and without LRB. The obtained analysis results are elaborately presented in terms of engineering demand parameters.

2. Analytical modelling and nonlinear analysis

The considered case study building is 20-storey moment resisting frame originally designed by [21] as high ductility level convenient with Eurocode 8 [22]. The storey height and bay width of the frame are 3.2 and 8 m, respectively, while the height is 4 m at the ground level. The beam and columns are subjected to the gravitational loading, graded with S275 and S355, designed with W sections, respectively, and illustrated in Fig. 3. The first period of the building is 3.75 sec. The building is assumed to be designed with peak ground acceleration of 0.35 g

and constructed in ground type B. The building importance factor and behavior factor are to be II and 6.5, respectively. The inherent damping ratio is considered as 3 %.

20-storey frame considered as fixed-base and then isolated with LRB (see Fig. 3(a) and (b)) considering the relevant standards like [3,22,23]. According to ASCE [24] and FEMA 356 [25], the plastic hinge mechanism is assumed to be formed at nodes of the beam and column. In addition, the panel zones and rigid diaphragm constraints are imposed for each storey for distributing the lateral forces proportionally to the structural members in the design of steel MRF. The nonlinear response of the fixed-base frame characterized with the lumped plasticity method. The modelling of the fixed-base and base-isolated frames are performed through finite element program of SAP2000 (2017) [26]. LRB has steel plates centered at the top and bottom of the bearing, also includes alternating layers, steel shims, and lead core located mid of the elastomeric plate as shown in Fig. 1 [9]. Authors selected the LRB as base isolation systems since the elastomeric rubber material is capable of lateral flexibility, the lead core contributes to the energy dissipation, the inner steel shims support the upcoming immense axial loads from high-rise building [27]. In the design of the base-isolated frame, LRB are modelled with nonlinear link element of "Rubber Isolator" because it perfectly describes the bilinear response (see Fig. 2) of the base isolators as recommended by [28-29].

The isolation parameters of LRB were determined considering the iterative method presented by [30]. First, the isolator displacement was assumed while the yield displacement was omitted, and then the iteration was to be proceeded until reached the presumed displacement value. The post yield stiffness ratio, is the ratio of the post-yield stiffness (k_1) to the initial stiffness (k_2), considered as 21 convenient with the study of [30]. LRB designed with isolation periods of 4, 4.5, and 5 sec. Thus, three base-isolated buildings have been developed to evaluate the isolator characteristics of LRB. The other isolation parameters were calculated and presented in Table 1.

Table 1. Properties of LRB for the outer columns of the base isolated frames

Variables	LRB (4 sec)	LRB (4.5 sec)	LRB (5 sec)
k_{eff} (kN/m)	1442.6	1139.8	641.1
W_d (kJ)	162.6	162.6	112.9
Q (kN)	119.4	106.1	66.3
k_2 (kN/m)	1097.4	867.1	487.7
D_y (mm)	5.4	6.1	6.8
D (m)	0.346	0.389	0.432
F_y (kN)	125.4	111.4	69.6

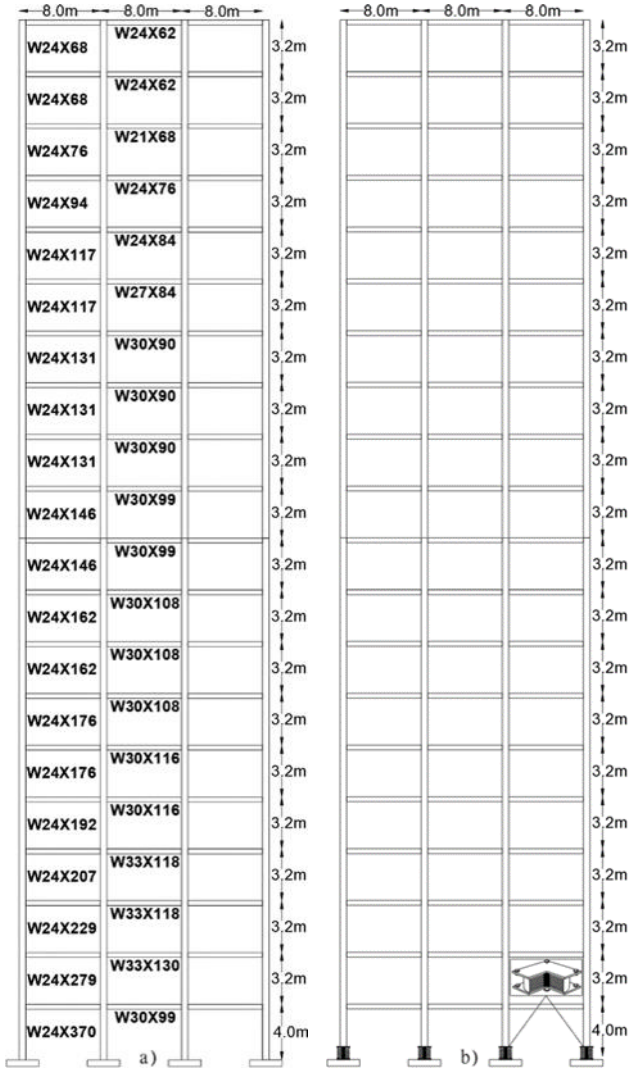

Figure 3. Elevation views of 20-storey; a) fixed-base [21] and b) LRB base-isolated frames

The force-displacement curve of the LRB (see Fig. 2) plotted by the following equations [30]

The effective stiffness, k_{eff};

$$k_{eff} = \frac{W}{g}.\left(\frac{2.\pi}{T}\right) \quad (1)$$

hysteresis loop (the energy dissipated per cycle), W_D;

$$W_D = 2.\pi.k_{eff}.\beta_{eff}.D \quad (2)$$

characteristics strength, Q;

$$Q = \frac{W_D}{4\left(D - D_y\right)} \quad (3)$$

post-yield stiffness of the isolator, k_2;

$$k_2 = k_{eff} - \frac{Q}{D} \quad (4)$$

yield displacement, Dy is given by;

$$D_y = \frac{Q}{(k_1 - k_2)} \quad (5)$$

effective period, Teff

$$T_{eff} = 2.\pi.\sqrt{\frac{W}{k_{eff}.g}} \quad (6)$$

damping reduction factor, B;

$$\frac{1}{B} = 0.25(1 - \ln\beta_{eff}) \quad (7)$$

displacement of isolation, D

$$D = \frac{g.S_a.{T_{eff}}^2}{B.4\pi^2} \quad (8)$$

and yield strength, Fy

$$F_y = Q + k_2.D_y \quad (9)$$

where target period is T, spectral acceleration is S_a, damping reduction factor is B, gravitational acceleration is g, characteristic strength is Q, total weight on the isolator is W, gravitational force is g, yield displacement is D_y, elastic stiffness is k_1, post-yield stiffness is k_2, and effective damping ratio is β_{eff}. The nonlinear response of the presented fixed-base and base-isolated high-rise steel frame models was evaluated by means of SAP 2000 (2017) by which the nonlinear time-history analyses were carried out with direct integration method. The earthquake records of Gazlı 1976, Tabas 1978, Cape Mendocino 1992, Chi-Chi 1999, and San Salvador 1986 presented in Table 2 were obtained from Pacific Earthquake Engineering Research Centre [31].

It is worthy to note that the force transmissibility of the LRB is an important issue and mainly depends on the ratio of dominating earthquake period to LRB base isolated building period. Based on the elastic design spectrum, the lengthening of the period could decrease the pseudo acceleration and therefore the earthquake induced forces in the buildings by increasing the deformation of the isolation systems. For the base isolation systems to be influential in diminishing the forces in the structures, isolated buildings period should be longer than the fixed base building period and similarly the dominant period of the ground motions [32].

Table 2. Characteristics of the ground motions used

Variables	Gazlı	Northridge	Chi-Chi	San Salvador	Supers. Hills
Year	1976	1994	1994	1987	1987
Station	Karakyr	Sylmar-Olive	TCU065	GeotechInvestig	Poe Road
Mechanism	Unknown	Reverse	R.-Oblique	Strike-Slip	Strike-Slip
M_w	6.8	6.69	7.62	5.8	6.54
R_{jb} (km)	3.9	0	0.6	2.1	0.9
R_{rup} (km)	5.5	5.3	0.6	6.3	0.9
V_{s30} (m/s)	659.6	251.2	305.9	545	348.7
PGA (g)	0.59	0.79	0.82	0.84	0.41
PGV (cm/s)	64.94	93.29	127.80	62.23	106.74
PGD (cm)	24.18	53.29	93.22	10.01	50.54

Note: Mw: Magnitude; Rjb: Surface projection distance; Rrup: Rupture distance; Vs30: Mean shear velocity over the top 30 m; PGA: Peak ground acceleration; PGV: Peak ground velocity; PGD: Peak ground displacement.

3. Results and Discussion

The seismic performance of the fixed-base and base-isolated high-rise steel buildings are investigated considering the effect of the isolation period on the nonlinear response of the lead rubber bearing through time history analyses. The analysis results are discussed in terms of storey displacement, isolator displacement, relative displacement, roof drift, interstorey drift ratio, absolute acceleration, base shear, base moment, input energy, and hysteretic curves.

20-storey fixed-base frame and base-isolated frame with LRB having the isolation periods of 4, 4.5, and 5 sec were tested through time history analyses within a series of ground motion records and those maximum storey displacements were presented in Fig. 4. The maximum storey displacement of the fixed-base frame under Gazlı earthquake was recorded as 100.3 cm, but fortunately it was reduced up to 55.7, 52.7, 51.2 cm by means of LRB with 4, 4.5, and 5 sec, respectively. The reduction effect of LRB on the storey displacement demand of the fixed-base frame was also testified when subjected to Northridge, Chi-Chi, Salvador, and Hills earthquakes. For example, the greatest reductions of 49, 14, 24, 28, and 23 % were experienced when 20-storey base-isolated frame with LRB having isolation period of 5 sec subjected to Gazlı, Northridge, Chi-Chi, Salvador, and Hills earthquakes, respectively. Similarly, the average maximum storey displacement of the fixed-base frame is recorded as 102.64 cm while it was as 77.9, 76.1, and 74.2

cm for the base-isolated frame with LRB of 4, 4.5, and 5 sec, respectively. It was noted that the excessive storey displacements of the fixed-based frame were alleviated by means of equipment of LRB having the greater isolation period.

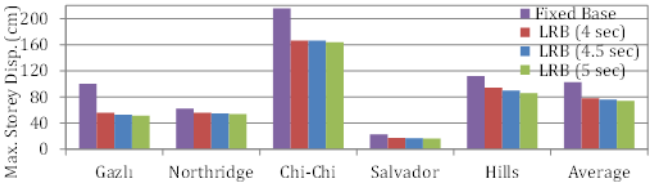

Figure 4. Maximum storey displacement of the case study frames under earthquakes

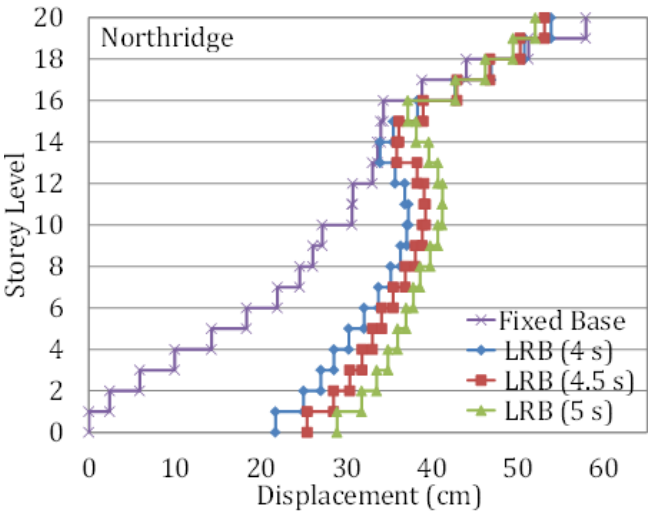

Figure 5. Variation of the storey displacement of the case study frames against storey height

The variation of the maximum storey displacements against storey height of high-rise frame with and without LRB under the effect of Northridge earthquake was illustrated in Fig. 5. The non-uniform storey distribution of the fixed-base frame was regulated if LRB was used. Compared to the lower isolation periods, LRB with 5 sec enhanced the storey displacement demand, in which the most uniform storey displacement pattern was experienced as well. However, the roof storey displacement of the fixed-base frame significantly reduced from 62.4 cm to 55.9, 54.9, and 53.7 cm corresponded to the reductions of 10, 12, 14 % for the isolation periods of 4, 4.5, and 5 sec, respectively.

The maximum isolator displacements of the base-isolated frames under earthquakes were presented in Fig. 6. The utilization of the greater isolation period in the design of LRB induced the lower stiffness for the bearing (see Table 1), thus the base-isolated frame can be easily swayed. For example, when subjected to Northridge earthquake, the maximum isolator displacements were obtained as 21.7, 25.4, and 28.9 cm for LRB with 4, 4.5, and 5 sec as shown in Fig. 6, those isolation periods corresponded to the effective stiffness of the bearing as 1442.6, 1139.8, and, 641.1 kN/m (see Table 1), respectively. As for the average maximum isolator displacement, similar trend was also recorded as 31.9, 35.4, and 38.5 cm (see Fig. 6), which was lower than the isolator displacement capacities as 34.6, 38.9, and 43.2 cm for LRB with 4, 4.5, and 5 sec (see Table 1), respectively.

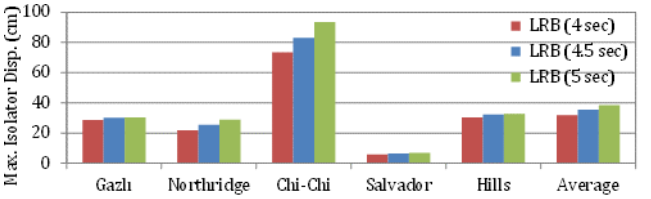

Figure 6. Maximum isolator displacement of the case study frames under earthquakes

The lateral displacement of any storey in the building with respect to the ground level was defined as relative displacement [33]. The maximum relative displacements of the case study frames were computed and presented in Fig. 7.

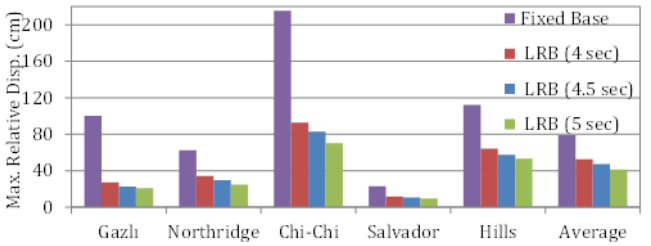

Figure 7. Maximum relative displacement of the case study frames under earthquakes

The utilization of LRB with 4 sec mitigated the excessive relative displacement of the fixed-base frame from 100.3 to 27.2 cm (73 %), 62.4 to 34.2 cm (45 %), 215.4 to 92.7 cm (57 %), 22.9 to 11.8 cm (48 %), 112.1 to 64.2 cm (42 %), furthermore the greatest reductions of LRB with 5 sec were recorded as 80, 60, 67, 58, and 53 % under Gazlı, Northridge, Chi-Chi, Salvador, and Hills earthquakes, respectively. The variation of the relative displacement height of the case study frames under Northridge earthquake was presented in Fig. 8. The relative displacements on the roof storey were as 62.4, 34.2, 29.6, and 24.9 cm for the fixed-base frame, isolated frame with 4, 4.5, and 5 sec, respectively. It can be seen LRB with the greater isolation period performed not only the more uniform pattern but also the lower relative displacement.

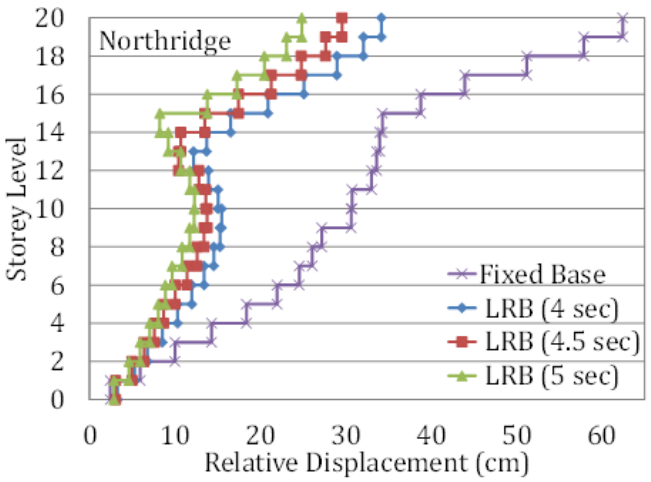

Figure 8. Variation of the relative displacement of the case study frames against storey height

The interstorey drift ratio is a significant index diagnosed the seismic performance of the buildings, which can be computed by subtracting the displacements of the adjacent storey and normalized by the storey height [34]. The maximum interstorey drift ratios of the fixed base frame and isolated frames with LRB were presented in Fig. 9. The former was as 2, 3, 2, 5, 1, and 4 % under Gazlı, Northridge, Chi-Chi, Salvador, and Hills earthquakes, however, they were reduced up to 1, 2, 3, 1, and 1 % by LRB with 5 sec, which corresponded to 64, 23, 44, 50, and 66 % reduction in the maximum interstorey drift ratio, respectively. Moreover, LRB with 4.5 sec provided the interstorey drift reductions as 56, 46, 21, 47, and 63 % compared to the fixed-base frame as shown in Fig. 8. The greatest reductions of 62, 63, and 66 % were observed when used LRB with 4, 4.5, and 5 sec under Hills earthquakes, respectively.

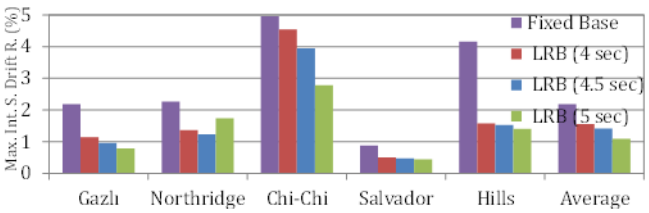

Figure 9. Maximum interstorey drift ratio of the case study frames under earthquakes

The effectiveness of the greater isolation period was also experienced in Fig. 10, which described the variation of the interstorey drift ratio with respect to the height of the case study frames under Northridge earthquake. The scattered interstorey drift pattern of the fixed-base frame was regulated by means of LRB. The most uniform interstorey drift ratio distribution was observed in LRB with the isolation period of 5 sec. The isolation period of 4.5 sec was tended to behave much more uniform trend especially in high-rise/upper storeys as shown in Fig. 10. It is worthy to note that the response of the structures under earthquakes depends on the fundamental period and the spectral acceleration of the ground motions corresponding to the periods, therefore, for different natural earthquakes varying responses were observed.

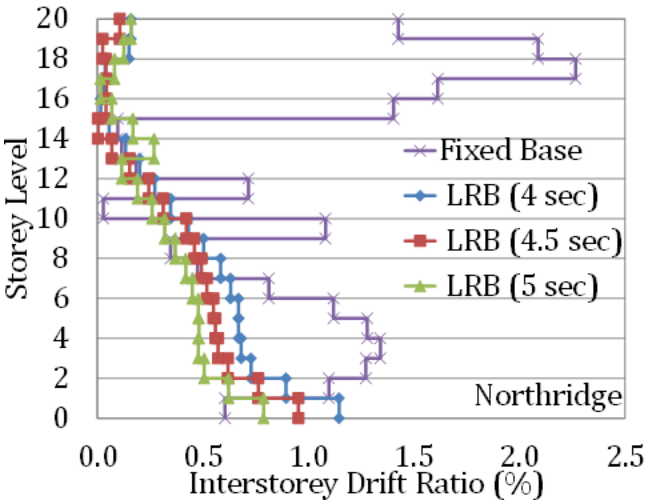

Figure 10. Variation of the interstorey drift ratio of the case study frames against storey height

The maximum absolute accelerations of the case study frames were given in Fig. 11. The fixed-base frame had by far the greatest absolute accelerations as 5.4, 7.2, 7.6, 9.1, and 6.4 m/s² when subjected to Gazlı, Northridge, Chi-Chi, Salvador, and Hills earthquakes, likewise they were reduced up to 3.7, 3.9, 3.5, 4.3, and 4.4 m/s², respectively, by means of LRB with 4 sec. The lowest maximum absolute acceleration of 2.8 m/s² was observed in case of LRB with 5 sec hit by Chi-Chi earthquake, which corresponded to 62 % reduction with respect to the considered fixed-base frame. It was as 54 and 59 % for LRB with 4 and 4.5 sec, respectively.

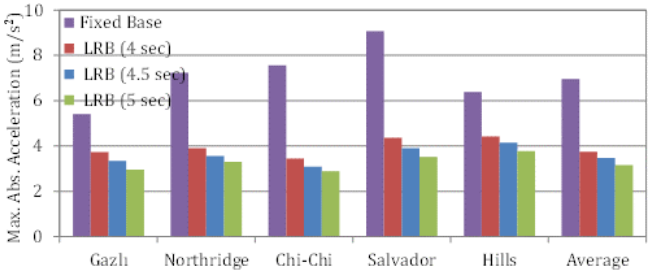

Figure 11. Maximum absolute acceleration of the case study frames under earthquakes

Fig. 12 described the variation of the absolute acceleration toward height of the case studied frames subjected to Northridge earthquake. Similar to the interstorey drift ratio variation, LRB having the greater isolation period tended to describe much more uniform absolute acceleration distribution. For example, the greatest storey acceleration was recorded as 7.2 m/s² at 14th storey, which mitigated to 2.1, 1.8, and 1.6 m/s² through LRB with 4, 4.5, and 5 sec, similarly, they performed the reductions as 39, 44, and 46 % at the roof storey absolute acceleration, respectively.

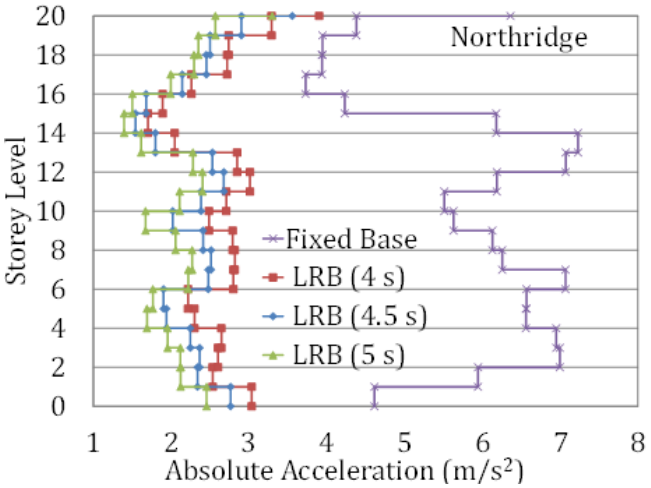

Figure 12. Variation of the absolute acceleration of the case study frames against storey height

The maximum base shears of the fixed base frame and isolated frames with LRB determined under earthquakes, and then normalized by building weight (32090 kN) were presented in Fig. 13. Compared to the fixed-base frame, LRB with 4 sec mitigated the base shears as 60, 63, 39, 66, and 54 %, and LRB with 5 sec satisfied the greatest reductions as 71, 68, 44, 73, and 67 % under Gazlı, Northridge, Chi-Chi, Salvador, and Hills

earthquakes, respectively. In addition, the average reductions were recorded as 54, 58, and 62 % through LRB with 4, 4.5, and 5 sec, respectively.

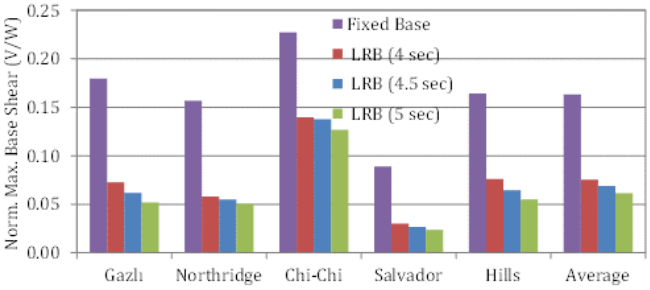

Figure 13. Maximum base shear of the case study frames under earthquakes

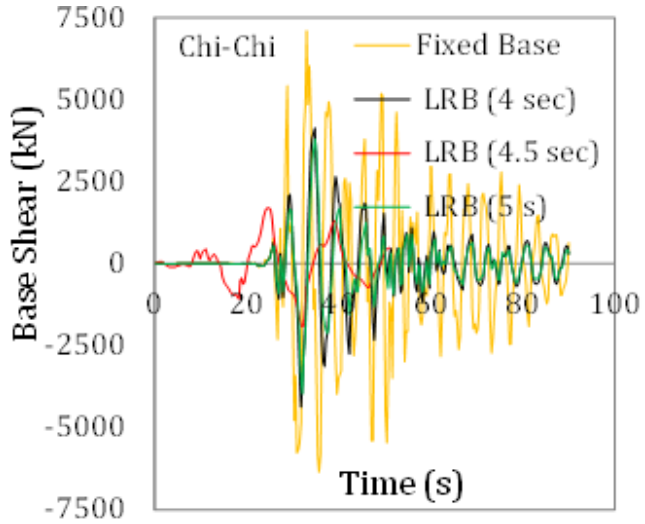

Figure 14. Time history response of base shear

The time history response of the base shear for the fixed-base frame and base-isolated frame with LRB having T of 4, 4.5, and 5 sec under the effect of Chi-Chi earthquake were presented in Fig. 14. The ranges of the base shear were observed to be between -6342 and 7097 kN, -4361 and 4139 kN, -4300 and 4194 kN, -3959 and 3807 kN for the fixed-base, LRB with 4, 4.5, and 5 sec respectively. It was shown that the utilization of the greatest isolation period was not only decreased the base shear but also narrowed the scatter time history response of the fixed-base.

Also, the maximum base moments were computed and presented in Fig. 15. Similar to the base shear demands, the use of LRB with 4 sec reduced the maximum base moment of the fixed-base frame as 57, 22, 30, 38, and 12 % when subjected to Gazlı, Northridge, Chi-Chi, Salvador, and Hills earthquakes, while they were as 71, 27, 41, 50, and 25 % for LRB with 5 sec, respectively.

The input energy dissipated by regular structural members (beam, column) for fixed-base frame, while the most of the input energy nearly 90 % consumed by energy dissipation device for the isolated frame. Therefore, the input energy of the base-isolated frame was much lower than that of fixed-base frame [35]. The input energy of the fixed-base frame and base-isolated frame with LRB were determined under earthquakes and presented in Fig. 16. The input energy of the base-isolated frames with LRB having greater isolation periods (i.e., 4.5 and 5 sec) was less than fixed-base frame and base-isolated frame with LRB of 4 sec. Compared to the fixed-base frame, LRB with 4.5 sec mitigated the input energy as 31, 18, 30, 20, and 8 % under Gazlı, Northridge, Chi-Chi, Salvador, and Hills earthquakes, respectively. As for LRB with 5 sec, the reductions were 38, 20, 42, 22, and 16 %, respectively.

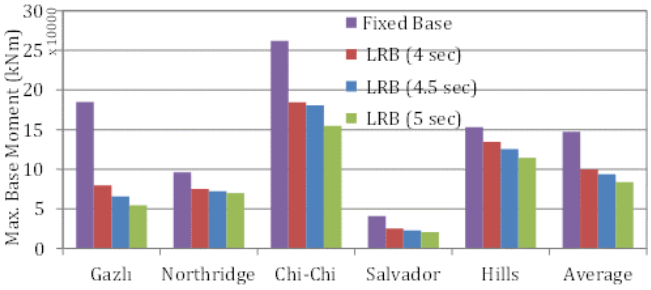

Figure 15. Maximum base moment of the case study frames under earthquakes

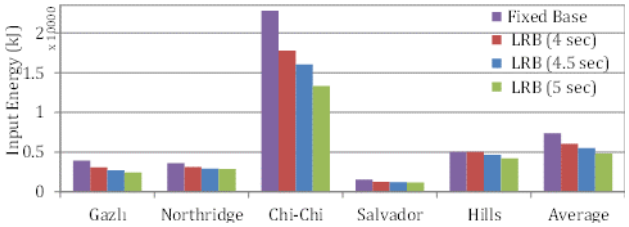

Figure 16. Input energy of the case study frames under earthquakes

When the fixed-base and base-isolated frames were hit by Chi-Chi earthquake, the time history responses of input energy were computed and presented in Fig. 17. The maximum input energies were recorded as 22808, 17767, 160033, and 13348 kJ for the fixed-base frame, base-isolated frame with LRB of 4, 4.5, and 5 sec, respectively.

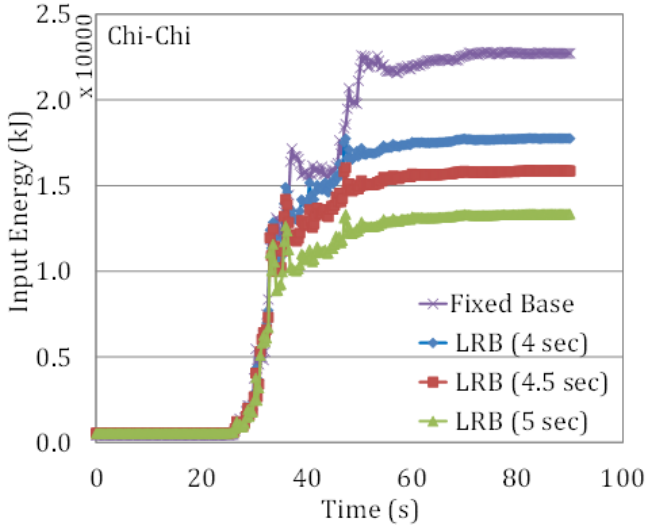

Figure 17. Time history response of input energy

The force-displacement cycles of the base-isolated frames with LRB of 4, 4.5, and 5 sec obtained through time-history analysis with Gazlı earthquake were presented in Fig. 18. The hysteretic curve of outer LRB with 4, 4.5, and 5 sec produced the yield forces (F_y) as

122.4, 110.6, and 82.5 kN proved the design values of the bearings (see Table 1). The maximum forces of 417.5, 346.6, 298.3 kN and the maximum isolator displacements of 0.285, 0.292, and 0.299 m were experienced in the base-isolated frames with LRB of 4, 4.5, and 5 sec under Gazlı earthquake, respectively.

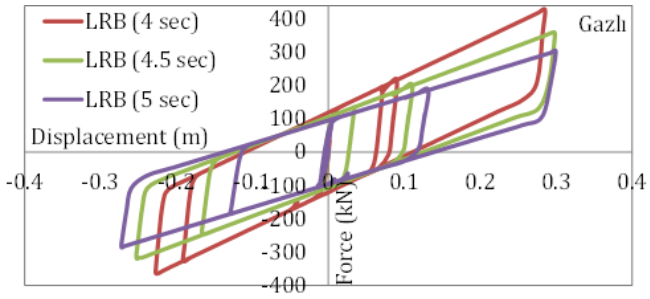

Figure 18. The force-displacement cycles of LRB with T of 4, 4.5, and 5 sec under Gazlı earthquake

4. Conclusion

Based on the results of the nonlinear analysis, a number of conclusions can be drawn as follows:

1. The use of greater isolation period reduced the lateral stiffness of LRB while the maximum storey displacements were significantly reduced. Compared to fixed-base frame, on average, the maximum displacement reductions occurred as 24, 26, and 28 % for the base-isolated frame with LRB of 4, 4.5, and 5 sec, respectively. The latter also successfully tended to behave the most uniform storey displacement.

2. The greatest average maximum isolator displacements were as 38.5 cm by the base-isolated frames with LRB of 5 sec.

3. The greatest reductions on the average maximum relative displacement were as 33, 40, and 48 % when high-rise frame isolated with LRB of 4, 4.5, and 5 sec, respectively. The greatest isolation period (T = 5 sec) presented the most uniform relative displacement distribution compared to the others.

4. The greater T not only reduced the maximum interstorey drift ratio but also showed the more uniform drift distribution. For example, LRB with T of 5 sec reduced in over half of the the average maximum interstorey drift ratio.

5. The use of LRB with 4, 4.5, and 5 sec mitigated the average maximum absolute acceleration as 46, 50, 55 %, respectively. LRB with T of 5 sec exhibited the best distribution pattern height of the base-isolated frames.

6. LRB with the greatest T was responsible both for mitigating the base shear and base moment as 62, 43 %, respectively.

7. The greatest average input energy mitigations of 18, 25, and 35 % were experienced when isolated with LRB with T of 4, 4.5, and 5 sec, respectively.

8. Among the ground motions, Chi-Chi being the most decisive earthquake revealed great difference response through LRB with 4, 4.5, and 5 sec, while Salvador earthquake was the steady.

9. The force-displacement cycles proved that the isolator could be displaced much more as T increased.

Author contributions

Ahmet Hilmi Deringöl: Conceptualization, Methodology, Software, Writing, Original draft preparation, Validation. **Esra Mete Güneyisi:** Visualization, Investigation, Writing-Reviewing and Editing.

Conflicts of interest

The authors declare no conflicts of interest.

References

1. Murru, M., Akinci, A., Falcone, G., Pucci, S., Console, R., & Parsons, T. (2016). M≥ 7 earthquake rupture forecast and time-dependent probability for the Sea of Marmara region, Turkey. *Journal of Geophysical Research: Solid Earth*, *121*(4), 2679-2707.
2. TEC-2007, Turkish Earthquake Code, Ministry of Public Works and Settlement, Republic of Turkey, Ankara.
3. TBEC 2018 – Turkish Building Earthquake Code 2018, Republic of Turkey Ministry of Interior Disaster and Emergency Management Presidency, Ankara, Turkey.
4. Xu, Y., Becker, T. C., & Guo, T. (2021). Design optimization of triple friction pendulums for high-rise buildings considering both seismic and wind loads. *Soil Dynamics and Earthquake Engineering*, *142*, 106568.
5. Markou, A. A., Stefanou, G., & Manolis, G. D. (2018). Stochastic response of structures with hybrid base isolation systems. *Engineering Structures*, *172*, 629-643.
6. Skinner, R. I., Robinson, W. H., & McVerry, G. H. (1993). *An introduction to seismic isolation*. Wiley.
7. Park, K. S., Jung, H. J., & Lee, I. W. (2002). A comparative study on aseismic performances of base isolation systems for multi-span continuous bridge. *Engineering Structures*, *24*(8), 1001-1013.
8. Kurino, S., Wei, W., & Igarashi, A. (2021). Seismic fragility and uncertainty mitigation of cable restrainer retrofit for isolated highway bridges incorporated with deteriorated elastomeric bearings. *Engineering Structures*, *237*, 112190.
9. Zordan, T., Liu, T., Briseghella, B., & Zhang, Q. (2014). Improved equivalent viscous damping model for base-isolated structures with lead rubber bearings. *Engineering Structures*, *75*, 340-352.
10. Ahmadipour, M., & Alam, M. S. (2017). Sensitivity analysis on mechanical characteristics of lead-core steel-reinforced elastomeric bearings under cyclic loading. *Engineering Structures*, *140*, 39-50.
11. Pant, D. R., Constantinou, M. C., & Wijeyewickrema, A. C. (2013). Re-evaluation of equivalent lateral force procedure for prediction of displacement demand in seismically isolated structures. *Engineering Structures*, *52*, 455-465.

12. Kazeminezhad, E., Kazemi, M. T., & Mirhosseini, S. M. (2020). Modified procedure of lead rubber isolator design used in the reinforced concrete building. *Structures*, 27, 2245-2273.
13. Deringöl, A. H., & Güneyisi, E. M. (2020). Effect of lead rubber bearing on seismic response of regular and irregular frames in elevation. *Pamukkale Üniversitesi Mühendislik Bilimleri Dergisi*, *26*(6), 1076-1085.
14. Shakouri, A., Amiri, G. G., & Salehi, M. (2021). Effects of ductility and connection design on seismic responses of base-isolated steel moment-resisting frames. *Soil Dynamics and Earthquake Engineering*, *143*, 106647.
15. Ye, K., Xiao, Y., & Hu, L. (2019). A direct displacement-based design procedure for base-isolated building structures with lead rubber bearings (LRBs). *Engineering Structures*, *197*, 109402.
16. Gupta, P. K., Ghosh, G., & Pandey, D. K. (2021). Parametric study of effects of vertical ground motions on base isolated structures. *Journal of Earthquake Engineering*, *25*(3), 434-454.
17. Habib, A., Houri, A. A., & Yildirim, U. (2021). Comparative study of base-isolated irregular RC structures subjected to pulse-like ground motions with low and high PGA/PGV ratios. *Structures*, 31, 1053-1071.
18. Altalabani, D., Hejazi, F., Rashid, R. S. B. M., & Abd Aziz, F. N. A. (2021). Development of new rectangular rubber isolators for a tunnel-form structure subjected to seismic excitations. *Structures*, 32, 1522-1542.
19. Zhang, R. J., & Li, A. Q. (2021). Experimental study on loading-rate dependent behavior of scaled high performance rubber bearings. *Construction and Building Materials*, *279*, 122507.
20. Deringöl, A. H., & Güneyisi, E. M. (2021). Effect of Using High Damping Rubber Bearings for Seismic Isolation of the Buildings. *International Journal of Steel Structures*, *21*(5), 1698-1722.
21. Karavasilis, T. L. (2016). Assessment of capacity design of columns in steel moment resisting frames with viscous dampers. *Soil Dynamics and Earthquake Engineering*, *88*, 215-222.
22. CEN, C. E. D. N. (2004). Eurocode 8: Design of structures for earthquake resistance Part 1. *General rules, seismic actions and rules for buildings (EN 1998–1), Brussels*.
23. American Society of Civil Engineers, ASCE. (2010). Minimum design loads for buildings and other structures. ASCE/SEI 7-10, Reston, VA.
24. ASCE 7-05. (2005). Minimum Design Loads for Buildings and Other Structures. American Society of Civil Engineers, Reston, Virginia.
25. FEMA (Federal Emergency Management Agency) (2000). Prestandard and commentary for the seismic rehabilitation of building. FEMA-356, D.C.
26. Computers and Structures, Inc. SAP 2000 v20.0.0 (2017). Static and dynamic finite element analysis of structures, Berkeley, California.
27. Markou, A. A., & Manolis, G. D. (2016). Mechanical models for shear behavior in high damping rubber bearings. *Soil Dynamics and Earthquake Engineering*, *90*, 221-226.
28. Park, Y. J., Wen, Y. K., & Ang, A. H. S. (1986). Random vibration of hysteretic systems under bi-directional ground motions. *Earthquake engineering & structural dynamics*, *14*(4), 543-557.
29. Wen, Y. K. (1976). Method for random vibration of hysteretic systems. *Journal of the engineering mechanics division*, *102*(2), 249-263.
30. Naeim, F., & Kelly, J. M. (1999). *Design of seismic isolated structures: from theory to practice*. John Wiley & Sons.
31. PEER (2011). The Pacific Earthquake Engineering Research Center. User's Manual for the PEER Ground Motion Database Application. Berkeley: University of California.
32. Chopra, A. K. (1995). Dynamics of Structures: Theory and Applications to Earthquake Engineering. Englewood Cliffs, N.J: Prentice Hall.
33. Guan, Y., Zhou, X., Yao, X., & Shi, Y. (2020). Seismic performance of prefabricated sheathed cold-formed thin-walled steel buildings: shake table test and numerical analyses. *Journal of Constructional Steel Research*, *167*, 105837.
34. Avila, L., Vasconcelos, G., Lourenço, P. B. (2018). Experimental study on loading-rate dependent behavior of scaled high performance rubber bearings. Engineering Structures, 155, 298–314.
35. Gajan, S., & Saravanathiiban, D. S. (2011). Modeling of energy dissipation in structural devices and foundation soil during seismic loading. Soil Dynamics and Earthquake Engineering, 31(8), 1106-1122.